Available online at www.sciencedirect.com
ScienceDirect
Optik 118 (2007) 289–295
Optik Optics
www.elsevier.de/ijleo

Hermite hyperbolic/sinusoidal Gaussian beams in *ABCD* systems

Halil Tanyer Eyyuboğlu*

Electronic and Communication Engineering Department, Çankaya University, Öğretmenler Cad. No:14 Yüzüncüyıl 06530 Balgat Ankara, Turkey

Received 24 October 2005; received in revised form 18 January 2006; accepted 23 March 2006

Abstract

For a Hermite hyperbolic/sinusoidal Gaussian beam with focusing properties, passing through an arbitrarily shaped rectangular aperture on the source plane and an on-axis x–y asymmetric *ABCD* system, the receiver plane expression is derived using the Collins integral. The specific example of a single thin lens placed on the propagation path is examined at selected source, propagation and optical element parameters. Viewing the progress of the beam in propagation, we find that subjecting the source beam to an aperture will give rise to excessive spreading during propagation. The lens setup will act to concentrate the energy of the beam around its focal point as expected, while in some circumstances it will also execute beam profile changes. By adjusting the aperture opening in the shape of a narrow slit, the beam will become aligned in the opposite direction after propagating after having traveled sufficiently. The results are presented as intensity graphs in the form of contour plots and 3D illustrations.

Keywords: *ABCD* systems; Propagation; Hermite hyperbolic/sinusoidal gaussian beams

1. Introduction

We have been analyzing the propagation characteristics of cosh-Gaussian [1], cosine-Gaussian [2] Hermite cosh-Gaussian [3], Hermite cosine-Gaussian [4], Hermite-sine-Gaussian and Hermite-sinh-Gaussian [5] beams in turbulent atmosphere. Our principle aim is to assess the suitability of these specialized beams as opposed to the pure Gaussian ones, i.e. the fundamental mode, for applications such as free space optical (FSO) links, laser radar, imaging and remote sensing. As a continuation of our endeavors in this direction, we present, in this study, the propagation of characteristics of a Hermite hyperbolic/sinusoidal Gaussian beam passing through an *ABCD* system. Our formulation is general in the sense that via the simple settings of the relevant parameters, one is able to generate the receiver field expression for all types of Hermite hyperbolic/sinusoidal Gaussian beams. Additionally the focusing properties of the source excitation as well as the on-path optical elements and their asymmetric attributions are included hereby, which is considered useful for practical applications of FSO, laser radar and imaging. Recently, in a different publication [6], the initial results of our investigations on the same topic were reported.

So far, the propagation characteristics for particular cases of Hermite hyperbolic/sinusoidal beams, in an *ABCD* system environment, have been investigated by several authors for on-axis and for off-axis situations. For instance, [7–10] deal with axial (on-axis) cases, while [11–13] cover the off-axis cases as well as simple Hermite–Gaussian beam type. Other specialized beams,

*Corresponding author. Tel.: +90 312 284 4500x360; fax: +90 312 284 8043.
E-mail address: h.eyyuboglu@cankaya.edu.tr.

0030-4026/$ - see front matter
doi:10.1016/j.ijleo.2006.03.022

namely Bessel–Gauss [14], Hermite–Laguerre–Gaussian [15], super-Gaussian [16], flat-topped Gaussian [17] and Gaussian Schell-model [18] beams have been examined in the context of *ABCD* systems, along with the consideration of multiple hard-edge aperture configurations [16,19].

In these studies, one dimensional co-centric square aperture construction is considered, while [7–13] deal with a specific selection from the family of Hermite hyperbolic/sinusoidal Gaussian beams without any focusing property. Furthermore in these studies, the lens placed on the propagation axis is assumed to have infinite transmission aperture and perfect rotational symmetry on the transverse plane. In this respect, the distinguishing features of our model can be summarized as follows:

(a) arbitrary source aperture construction in rectangular geometry,
(b) ability to handle the whole set of Hermite hyperbolic/sinusoidal Gaussian beams with focusing properties under one single formulation,
(c) capability to account for asymmetric *x-y* situations both along the propagation axis and in the optical elements on the way.

2. Formulation

The source field, $u_s(\mathbf{s}) = u_s(s_x, s_y)$, is expressed as

$$u_s(\mathbf{s}) = A_c H_n(a_x s_x + b_x) H_m(a_y s_y + b_y) \times \exp\left[-0.5k\left(\alpha_x s_x^2 + \alpha_y s_y^2\right)\right] \times \{l_1 \exp[\mathrm{j}(V_x s_x + V_y s_y)] + l_2 \times \exp[\mathrm{j}(Y_x s_x + Y_y s_y)]\} \quad (1)$$

(s_x, s_y) denote the decomposition of the vector $\mathbf{s}$ into x and y components. A_c is the amplitude factor of the source field and will be taken as unity from this point onwards, $H_n(a_x s_x + b_x)$ and $H_m(a_y s_y + b_y)$ are Hermite polynomials describing the beam distribution for s_x and s_y directions, where n and m are the order, a_x and a_y stand for the width, b_x and b_y are the complex displacement parameters

$$\alpha_x = 1/(k\alpha_{sx}^2) + \mathrm{j}/F_{sx}, \quad \alpha_y = 1/\left(k\alpha_{sy}^2\right) + \mathrm{j}/F_{sy} \quad (2)$$

α_{sx} and α_{sy} are Gaussian source sizes, F_{sx} and F_{sy} are the source focusing parameters along s_x and s_y directions, $k = 2\pi/\lambda$ is the wave number with λ being the wavelength and $j = (-1)^{0.5}$. The parameters l_1, l_2, V_x, V_y, Y_x and Y_y are associated with the hyperbolic/sinusoidal attribution of the beam such that, their appropriate assignments will generate cosh-Gaussian, cosine-Gaussian, sinh-Gaussian and sine-Gaussian beams as explained in [5].

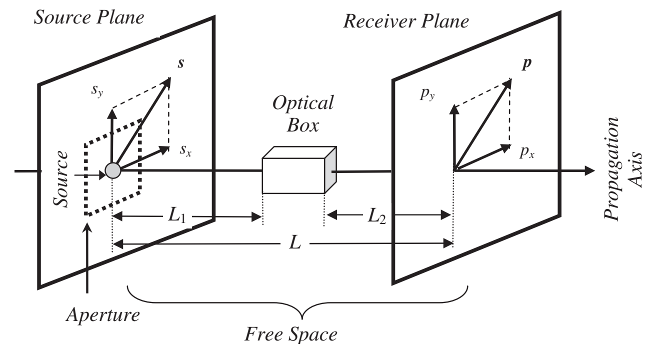

Fig. 1. Propagation geometry.

The beam that originates from the source field supplied by Eq. (1), after traveling in the free space environment containing optical items as depicted in Fig. 1, will be incident on a receiver plane located at an axial distance of L. There, the receiver field, $u_r(\mathbf{p}) = u_r(p_x, p_y)$, is to be evaluated with the help of Collins integral (also known as Huygens–Fresnel diffraction integral) in the manner stated below

$$u_r(\mathbf{p}) = -\mathrm{j}k/\left(2\pi B_x^{0.5} B_y^{0.5}\right) \int_{t_{y1}}^{t_{y2}} \int_{t_{x1}}^{t_{x2}} d^2\mathbf{s} u_s(\mathbf{s}) \times \exp\Big\{0.5\mathrm{j}k\Big[A_x s_x^2/B_x + A_y s_y^2/B_y - 2\left(s_x p_x/B_x + s_y p_y/B_y\right) + D_x p_x^2/B_x + D_y p_y^2/B_y\Big]\Big\}. \quad (3)$$

Since our optical items are thin lens type and there are no misalignments of refraction objects or the axes, the integrand of Eq. (3) is written purely in decoupled x and y subscripted quantities. Under such circumstances, the G and H elements of the *ABCDGH* matrix disappear as clarified in [20–22].

It is understood from Fig. 1, $\mathbf{p}$ is the positional vector on the receiver plane. The terms, t_{x1}, t_{x2}, t_{y1} and t_{y2} governing the integral limits for s_x and s_y direction refer to the dimensions of a rectangular aperture that may be placed on an arbitrary position of the source plane (see also Figs. 2, 4 and 5). The parameters A_x, A_y, B_x, D_x and D_y are the respective x and y elements of the *ABCD* matrix defining the optical content of the involved propagation geometry, such that if the box illustrated in Fig. 1 were to be a single thin lens characterized by the parameter α_{lx}, then the following matrix would hold for the entire link from source to receiver:

$$\begin{pmatrix} A_x & B_x \\ C_x & D_x \end{pmatrix} = \begin{pmatrix} 1 + \mathrm{j}\alpha_{lx}L_2 & L_1 + L_2(1 + \mathrm{j}\alpha_{lx}L_1) \\ \mathrm{j}\alpha_{lx} & 1 + \mathrm{j}\alpha_{lx}L_1 \end{pmatrix}. \quad (4)$$

An equivalent expression exists for the y components. The *ABCD* system is able to account for any number of

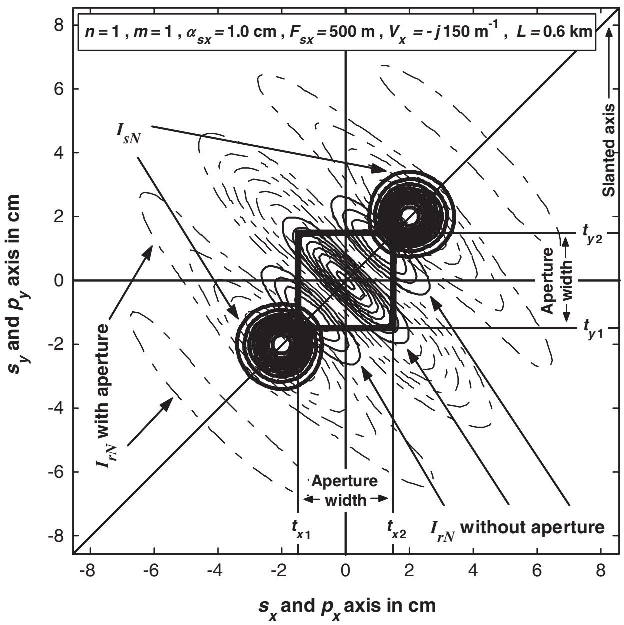

Fig. 2. Overlaid contour plot of three Hermite-cosh-Gaussian beams, one at source plane, the other without aperture at $L = 600\,\text{m}$, the last one is with aperture again at $L = 600\,\text{m}$.

cascaded sections with different compositions. Thus, Eq. (4) is obtained by multiplying the individual *ABCD* matrix representation of each section, namely L_1, the lens and L_2, in the reverse order [23]. The parameters α_{lx} and correspondingly α_{ly} are related to effective transmission apertures, α_{ax} and α_{ay} and focal lengths, F_{lx} and F_{ly}, of the thin lens via

$$\alpha_{lx} = 1/\left(k\alpha_{ax}^2\right) + \mathrm{j}/F_{lx}, \quad \alpha_{ly} = 1/\left(k\alpha_{ay}^2\right) + \mathrm{j}/F_{ly}. \tag{5}$$

In solving the Collins integral, first Eq. (1) is substituted for $u_s(\mathbf{s})$ in Eq. (3), then all Hermite polynomials are expanded in series, leaving hyperbolic/sinusoidal parameters of l_1, l_2, V_x, V_y, Y_x, Y_y and *ABCD* matrix elements in their unspecified state, a term by term integration based on the derivation steps outlined in the Appendix is performed, in the end, leading to the following result:

$$\begin{aligned} u_r(\mathbf{p}, z = L) = & -[\mathrm{j}k/(2\pi B)]\exp\left[0.5\mathrm{j}k\left(D_x p_x^2/B_x + D_y p_y^2/B_y\right)\right] \\ & \times \left\{ l_1 \exp\left[-0.5F_{sx}\alpha_{sx}^2 Q_{Vx}^2/(B_x Q_{Ax})\right] \right. \\ & \times \exp\left[-0.5F_{sy}\alpha_{sy}^2 Q_{Vy}^2/\left(B_y Q_{Ay}\right)\right] S_{Vx} S_{Vy} \\ & + l_2 \exp\left[-0.5F_{sx}\alpha_{sx}^2 Q_{Yx}^2/(B_x Q_{Ax})\right] \\ & \left. \times \exp\left[-0.5F_{sy}\alpha_{sy}^2 Q_{Yy}^2/\left(B_y Q_{Ay}\right)\right] S_{Yx} S_{Yy} \right\}, \end{aligned} \tag{6}$$

where

$$\begin{aligned} S_{Vx} = & \sum_{l_{x1}=0}^{[0.5n]} (-1)^{l_{x1}} 2^{n-l_{x1}} T_{lx1} \binom{n}{2l_{x1}} \\ & \times \sum_{l_{nx1}=0}^{n-2l_{x1}} (b_x)^{n-2l_{x1}-l_{nx1}} \binom{n-2l_{x1}}{l_{nx1}} \\ & \times (a_x)^{l_{nx1}} \left(\mathrm{j}F_{sx}\alpha_{sx}^2 Q_{Vx}/Q_{Ax}\right)^{l_{nx1}} \frac{l_{nx1}!}{2\left[0.5Q_{Ax}/\left(B_x F_{sx}\alpha_{sx}^2\right)\right]^{0.5}} \\ & \times \sum_{k_{x1}=0}^{l_{nx1}} \frac{\left(0.5\mathrm{j}Q_{Vx}/B_x\right)^{-k_{x1}} \left[0.5Q_{Ax}/\left(B_x F_{sx}\alpha_{sx}^2\right)\right]^{0.5k_{x1}}}{k_{x1}!(l_{nx1}-k_{x1})!} \\ & \times \left(\sum_{k_{x2}=0}^{[0.5(k_{x1}-1)]} \frac{(k_{x1}-1)!!}{2^{k_{x2}}(k_{x1}-1-2k_{x2})!!} \right. \\ & \times \left\{ g_{x1}^{k_{x1}-1} \exp\left[\frac{-0.5}{B_x F_{sx}\alpha_{sx}^2 Q_{Ax}}\left(t_{x1}Q_{Ax} - \mathrm{j}F_{sx}\alpha_{sx}^2 Q_{Vx}\right)^2\right] \right. \\ & \times \left[\frac{0.5}{B_x F_{sx}\alpha_{sx}^2 Q_{Ax}}\left(t_{x1}Q_{Ax} - \mathrm{j}F_{sx}\alpha_{sx}^2 Q_{Vx}\right)^2\right]^{0.5(k_{x1}-1)-k_{x2}} \\ & - g_{x2}^{k_{x1}-1} \exp\left[\frac{-0.5}{B_x F_{sx}\alpha_{sx}^2 Q_{Ax}}\left(t_{x2}Q_{Ax} - \mathrm{j}F_{sx}\alpha_{sx}^2 Q_{Vx}\right)^2\right] \\ & \left. \times \left[\frac{0.5}{B_x F_{sx}\alpha_{sx}^2 Q_{Ax}}\left(t_{x2}Q_{Ax} - \mathrm{j}F_{sx}\alpha_{sx}^2 Q_{Vx}\right)^2\right]^{0.5(k_{x1}-1)-k_{x2}} \right\} \\ & - \pi^{0.5} \frac{(k_{x1}-1)!!}{2^{0.5k_{x1}}} |\mathrm{rem}(k_{x1}-1, 2)| \\ & \times \left\{ \mathrm{erf}\left[\left(\frac{0.5}{B_x F_{sx}\alpha_{sx}^2 Q_{Ax}}\right)^{0.5}\left(t_{x1}Q_{Ax} - \mathrm{j}F_{sx}\alpha_{sx}^2 Q_{Vx}\right)\right] \right. \\ & \left.\left. - \mathrm{erf}\left[\left(\frac{0.5}{B_x F_{sx}\alpha_{sx}^2 Q_{Ax}}\right)^{0.5}\left(t_{x2}Q_{Ax} - \mathrm{j}F_{sx}\alpha_{sx}^2 Q_{Vx}\right)\right] \right\} \right). \end{aligned} \tag{7}$$

From Eq. (7), S_{Vy} is attained by changing all x subscripts to y and ns′ to ms′. S_{Yx} is the same as S_{Vx} except that all V_x s′ are to be replaced by Y_x s′. Finally S_{Yy} is identical to S_{Vy} except that all V_y s′ are to be replaced by Y_y s′. The definitions for the rest of the terms appearing in Eq. (7) are

$$\begin{gathered} Q_{Vx} = B_x V_x - kp_x, Q_{Vy} = B_y V_y - kp_y, \\ Q_{Yx} = B_x Y_x - kp_x, Q_{Yy} = B_y Y_y - kp_y, B = \left(B_x B_y\right)^{0.5}, \\ Q_{Ax} = B_x F_{sx} + \mathrm{j}k\alpha_{sx}^2(B_x - A_x F_{sx}), \\ Q_{Ay} = B_y F_{sy} + \mathrm{j}k\alpha_{sy}^2\left(B_y - A_y F_{sy}\right) \end{gathered} \tag{8}$$

g_{x1} and g_{x2} will take on the values +1 or –1 determined by the following conditions:

$$\begin{aligned} & g_{x1} = +1, g_{x2} = +1 \text{ when } \mathrm{real}\left(\mathrm{j}F_{sx}\alpha_{sx}^2 Q_{Vx}/Q_{Ax}\right) \leqslant t_{x1} < t_{x2}, \\ & g_{x1} = -1, g_{x2} = +1 \text{ when } t_{x1} < \mathrm{real}\left(\mathrm{j}F_{sx}\alpha_{sx}^2 Q_{Vx}/Q_{Ax}\right) < t_{x2}, \\ & g_{x1} = -1, g_{x2} = -1 \text{ when } t_{x1} < t_{x2} \leqslant \mathrm{real}\left(\mathrm{j}F_{sx}\alpha_{sx}^2 Q_{Vx}/Q_{Ax}\right) \end{aligned} \tag{9}$$

real(x) retrieves the real part of x, ! means the factorial notation, $(k)!! = 1x3x \ldots (k-1)$ or $(k)!! = 2x4x \ldots (k\text{-}1)$ depending on whether k is odd or even. The square brackets appearing in the upper limit of some summations in Eq. (7) indicate that the integral part of the enclosing expression is to be taken. The operator, rem(k, 2) generates the remainder of k when divided by 2. The sign $|x|$ implements the absolute value operation on x. Binomial coefficients are shown in the forms of $\begin{pmatrix} C_1 \\ C_2 \end{pmatrix}$ such that $\begin{pmatrix} C_1 \\ C_2 \end{pmatrix} = C_1!/[(C_1 - C_2)!C_2!]$, $T_{lx1} = 1 \times 3 \times \cdots \times (2l_{x1} - 1)$ for $l_{x1} \neq 0$, erf(.) is the error function.

Normally we are interested in the intensity at receiver plane. This is invoked by multiplying the receiver field with its conjugate, hence

$$I_r(\mathbf{p}) = u_r(\mathbf{p})u_r^*(\mathbf{p}), \tag{10}$$

where * stands for the conjugate.

3. Results and discussions

In this section, using Eqs. (1) and (10), we plot our results in the form of intensity graphs against the variations of source, optical element and propagation parameters, where the two last items are largely embedded into the elements of the *ABCD* matrix. To achieve this, the conversion of the source field into intensity expression is required, thus

$$I_s(\mathbf{s}) = u_s(\mathbf{s})u_s^*(\mathbf{s}). \tag{11}$$

In order to off-set the amplitude imbalances between the different calculations and obtain more interpretable illustrations, the following normalizations are established:

$$\begin{aligned} I_{sN}(\mathbf{s}) &= I_s(\mathbf{s})/\max[I_s(\mathbf{s})], \\ I_{rN}(\mathbf{p}) &= I_r(\mathbf{p})/\max[I_s(\mathbf{s})], \end{aligned} \tag{12}$$

where the operator max will furnish the peak value of the source intensity.

In all our exhibits, except the last one that is accompanied by the appropriate remarks, equivalent x and y indexed parameters are utilized. Therefore, for graphs of such cases, only the numeric values of x parameters are quoted with the understanding that y values are identical. For Hermite polynomials, the width parameters are equated to the inverse of the respective Gaussian source sizes, while the displacement factors are taken as zero, this means, $a_x = 1/\alpha_{sx}$, $a_y = 1/\alpha_{sy}$, $b_x = b_y = 0$. To allow the generation of any type of beam amongst the Hermite hyperbolic/sinusoidal Gaussian combinations, the settings of l_1, l_2, V_x, V_y, Y_x, and Y_y are adjusted according to the criteria listed in [5].

Although, it is possible with our formulation via the individual settings of t_{x1}, t_{x2}, t_{y1} and t_{y2} in Eqs. (3) and (7), to design an aperture having unequal sides within the negative and positive regions of the source transverse plane, in the scope of the present study, we only exemplify cases, for which the origin of the aperture is aligned to be co-centric with the origin of the source plane. All throughout the graphs, the wavelength of propagation is taken to be $\lambda = 1.55\,\mu$m.

By letting $l_1 = l_2 = 0.5$, $V_x = V_y = -\mathrm{j}150\,\mathrm{m}^{-1}$, $Y_x = Y_y = \mathrm{j}150\,\mathrm{m}^{-1}$, hence adopting a Hermite-cosh-Gaussian beam, with other source and propagation parameters being designated as shown in the inset, Fig. 2 displays the contour plot of three overlaid beams, namely, one at the source plane, the other at $L = 600$ m without any aperture confinements, the last one being at the same distance, but with an aperture of the marked dimensions. As seen from Fig. 2, due to magnitude of the source focusing parameters, that is $F_{sx} = F_{sy} = 500$ m, the intensity pattern at $L = 600$ m is narrower than that of the source plane, although the conversion towards a Hermite-cosine-Gaussian beam is already being experienced [3,4]. On the other hand, the beam passing through a square aperture, whose side is three times the Gaussian source size of the beam, becomes substantially more spread out after having traveled a distance of 600 m. This is to be expected, since this kind of aperture captures only a small slice of the source beam effectively lowering its transmitted source size, thus causing more spreading at the same propagation distance. We should point out that the computation of Fig. 2 has been accomplished assuming free space propagation with no on-path optical elements, in which case the *ABCD* matrix is

$$\begin{pmatrix} A_x & B_x \\ C_x & D_x \end{pmatrix} = \begin{pmatrix} A_y & B_y \\ C_y & D_y \end{pmatrix} = \begin{pmatrix} 1 & L \\ 0 & 1 \end{pmatrix}. \tag{13}$$

Fig. 3 provides the 3D view of the beam progress along the propagation axis, where the source plane aperture is totally removed. In the arrangement of Fig. 3, the beam, after being launched from the source plane, initially passes through a thin lens whose properties are given in the inset of the third picture, its image then falls onto a plane closely situated behind the lens. The parameters of this figure are almost the same as those of Fig. 2, except the mode indices are changed from $n = m = 1$ to $n = 1$, $m = 0$ and the beam type is switched from Hermite-cosh-Gaussian to Hermite-sinh-Gaussian, whilst the propagation range is doubled. The lens in question has $\alpha_{ax} = \alpha_{ay} = 5$ cm, $F_{sx} = F_{sy} = 5$ cm, being aligned to be co-centric with the axis of propagation and held perpendicular to it, at a distance of $L_1 = 1.2$ km from the source plane. An image (receiver) plane is placed at $L_2 = 6$ cm further away from the lens. Comparing the second and the third pictures of Fig. 3,

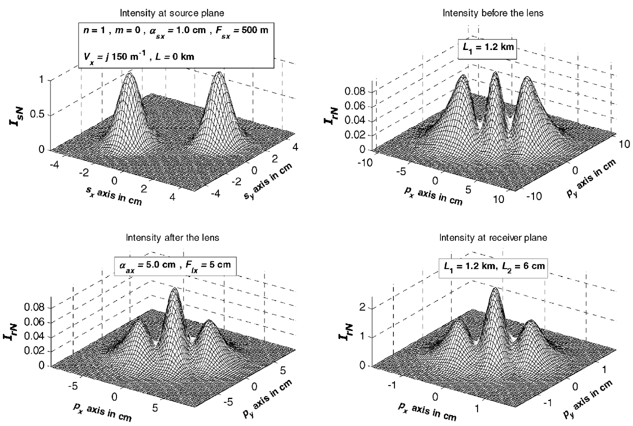

Fig. 3. Progress of a Hermite-sinh-Gaussian beam along the propagation axis with no aperture on the source plane.

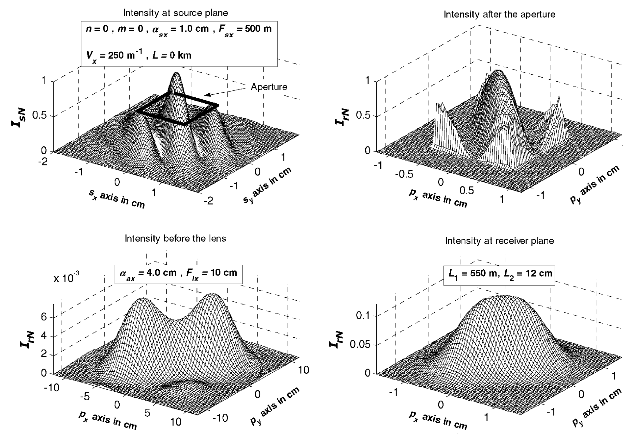

Fig. 4. Progress of a cosine-Gaussian beam along the propagation axis with aperture on the source plane.

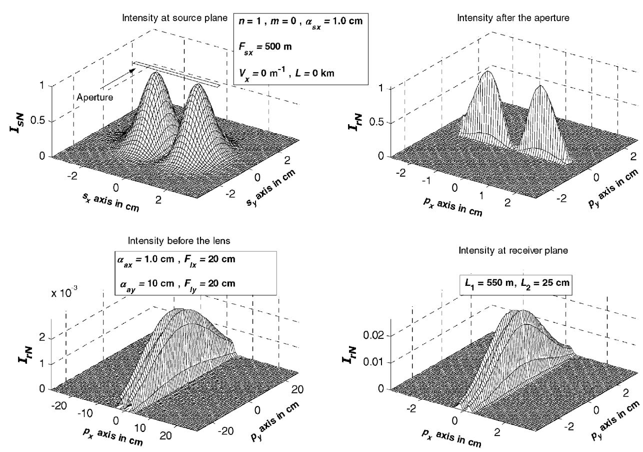

Fig. 5. Progress of a TEM_{10} beam along the propagation axis with a slit aperture on the source plane.

it is observed that, due to its finite size, the lens cannot capture all the energy in the incident beam, hence the profile is slightly altered. At a distance of 6 cm away from the lens however (fourth picture), being dominated by the act of focusing, the normalized peak intensity is greatly increased reaching twice that of the source. It is worth emphasizing that, the receiver plane intensity of the Hermite-sinh-Gaussian beam in Fig. 3 has now evolved towards Hermite-cosine-Gaussian profile, since the sum of mode indices, i.e. $n+m=1$, is odd [6].

Next we consider a sinusoidal type of Hermite–Gaussian beam, this time with the aperture reintroduced. A source beam possessing a central lobe is preferred, and to maximize this portion, the fundamental Hermite-cosine-Gaussian beam is opted for, that is $n = m = 0$. Using the source and propagation parameter values given in the insets, Fig. 4 illustrates the passage of the selected beam along the propagation axis, where in the first picture, i.e. the source plane, the borders of the employed square aperture, whose sides are 1.3 times the Gaussian source size, are also marked. The second picture of Fig. 4 is the intensity immediately after the aperture, showing how the hard aperture structure has performed a knife cut slicing on the original intensity profile. In the third picture, we see on one hand, the intermediate step of the intensity becoming cosh-Gaussian, on the other, the excessive amount of spreading caused by the aperture effects, despite the source focusing capability. This spreading is similar to the one witnessed in Fig. 2. Finally after passing through the thin lens, the original cosine-Gaussian beam turns into a pure Gaussian like shape, as observed from the last picture of Fig. 4.

The last scenario examines the behavior of beams in asymmetric conditions. Firstly, by letting $n=1$, $m=0$, $l_1=l_2=0.5$, $V_x=V_y=Y_x=Y_y=0$, the source beam is transformed into a TEM_{10} mode. Then, while on the source plane, this beam is allowed to pass through an aperture, which is as wide as 4 times the Gaussian source size along the s_x axis and 0.2 times the Gaussian source size in the s_y direction. Looking at Fig. 5, that shows the complete process of this particular beam along the propagation axis, we see that, having passed through such an aperture structure, the beam profile becomes akin to a single wing of the cross beam studied in [24]. In conformance with the findings of [24], after traveling sufficiently, as the third picture of Fig. 5 reveals, the beam becomes aligned in the opposite direction, which in this specific case is the p_y axis, in addition to the natural spreading phenomena. By employing a lens equipped with appropriate α_{ax}, α_{ay}, F_{lx} and F_{ly} assignments, it becomes possible to capture and focus the beam as shown in the forth picture of Fig. 5.

4. Conclusion

We have investigated the propagation characteristics of a Hermite hyperbolic/sinusoidal Gaussian beam with focusing capability in a free space environment consisting of arbitrary rectangular shaped source plane aperture and an on-axis thin lens with asymmetric properties. It is found that, the aperture effects will rise to more spreading. The previously observed conversion rules between different types of Hermite hyperbolic/sinusoidal Gaussian beams are still applicable. The lens will serve to capture part of the beam within its transmission aperture, focusing it to increase the peak intensity.

For future work, we aim to extend our treatment to more complicated cases like apertures placed on the path of axis away from the source plane, a multi optical element situation, which will have to take into consideration the thickness of the related objects and misalignments. Inclusion of atmospheric turbulence into this environment would also be another subject of our future investigations.

Acknowledgment

The author wishes to thank Emre Sermutlu, staff member of Mathematics and Computer Department of Çankaya University, for the basic solution of the integral in Eq. (A.1).

Appendix

In this appendix, the derivations steps from Eqs. (3) to (6) are somewhat elaborated.

After writing the series expansion for Hermite polynomials, the integral in Eq. (3) transforms into a simplified form of

$$I = \int_a^b x^n \exp\left(-px^2 + 2qx\right) \mathrm{d}x. \tag{A.1}$$

For finite limits of a and b, there is no readily available in the literature for Eq. (A.1), for this reason we have had to resort to the method of integration by parts. Solving Eq. (A.1) as an indefinite integral, then inserting the limits, an analytic result is delivered, where the various terms demonstrate conditional dependency on the parameters a, b, p and q as given below

$$\begin{aligned} I = {} & \exp\left(q^2/p\right)\left(q/p\right)^n \frac{n!}{2p^{0.5}} \sum_{k_1=0}^{n} \frac{q^{-k_1} p^{0.5k_1}}{k_1!(n-k_1)!} \\ & \times \left(\sum_{k_2=0}^{[0.5(k_1-1)]} \frac{(k_1-1)!!}{2^{k_2}(k_1-1-2k_2)!!} \left\{ g_1^{k_1-1} \right.\right. \\ & \times \exp\left[-p\left(a-q/p\right)^2\right] \left[p\left(a-q/p\right)^2\right]^{0.5(k_1-1)-k_2} \\ & - g_2^{k_1-1} \exp\left[-p\left(b-q/p\right)^2\right] \\ & \left. \times \left[p\left(b-q/p\right)^2\right]^{0.5(k_1-1)-k_2} \right\} \\ & - \pi^{0.5} \frac{(k_1-1)!!}{2^{0.5k_1}} |\mathrm{rem}(k_1-1,2)| \left\{ \mathrm{erf}\left[p^{0.5}\left(a-q/p\right)\right] \right. \\ & \left.\left. - \mathrm{erf}\left[p^{0.5}\left(b-q/p\right)\right] \right\} \right), \end{aligned}$$

$$\begin{aligned} & g_1 = +1, g_2 = +1, \text{ when } q/p \le a < b \\ & g_1 = -1, g_2 = +1, \text{ when } a < q/p < b, \\ & g_1 = -1, g_2 = -1, \text{ when } a < b \le q/p. \end{aligned} \tag{A.2}$$

Upon inspection, it is realized that, the conditions listed above are essentially the same as those stated in the main text. We may verify that in the limit of $a \to \infty$ and $a \to \infty$, (A.2) will reduce to Eq. (3.462.2) of [25].

Since, there is no coupling between s_x and s_y, applying Eq. (A.2) to (3) twice individually, one finally arrives at Eq. (6).

References

[1] H.T. Eyyuboğlu, Y. Baykal, Average intensity and spreading of cosh-Gaussian laser beams in the turbulent atmosphere, Appl. Opt. 44 (6) (2005) 976–983.
[2] H.T. Eyyuboğlu, Y. Baykal, Analysis of reciprocity of cos-Gaussian and cosh-Gaussian laser beams in a turbulent atmosphere, Opt. Express 12 (20) (2004) 4659–4674.
[3] H.T. Eyyuboğlu, Propagation of Hermite-cosh-Gaussian laser beams in turbulent atmosphere, Opt. Commun. 245 (1–6) (2005) 37–47.
[4] H.T. Eyyuboğlu, Hermite-cosine-Gaussian laser beam and its propagation characteristics in turbulent atmosphere, J. Opt. Soc. Am. A 22 (8) (2005) 1527–1535.
[5] H.T. Eyyuboğlu, Y. Baykal, Hermite-sine-Gaussian and Hermite-sinh-Gaussian laser beams in turbulent atmosphere, J. Opt. Soc. Am. A 22 (12) (2005) 2709–2718.
[6] H.T. Eyyuboğlu, Propagation of a generalized beam in ABCD system, in: Proceedings of Enformatika, Prague, 2005, pp. 211–216.
[7] A. Belefhal, M. Ibnchaikn, Propagation properties of Hermite-cosh-Gaussian laser beams, Opt. Commun. 186 (4–6) (2000) 269–276.
[8] S. Yu, H. Guo, X. Fu, W. Hu, Propagation properties of elegant Hermite-cosh-Gaussian laser beams, Opt. Commun. 204 (1–6) (2002) 59–66.
[9] N. Zhou, G. Zeng, Propagation properties of Hermite-cosine-Gaussian beams through a paraxial optical *ABCD* system with hard-edge aperture, Opt. Commun. 232 (1–6) (2004) 49–59.
[10] Y. Qui, H. Guo, X. Chen, H.J. Kong, Propagation properties of an elgant Hermite-cosh-Gaussian beams through a finite aperture, J. Opt. A: Pure Appl. Opt. 6 (2) (2004) 210–215.

[11] B. Lü, H. Ma, Coherent and incoherent off-axis Hermite–Gaussian beam combinations, Appl. Opt. 39 (8) (2000) 1279–1289.
[12] D. Zhao, H. Mao, W. Zhang, S. Wang, Propagation of off-axial Hermite-cosine-Gaussian beams through an apertured and misaligned *ABCD* optical system, Opt. Commun. 224 (1–3) (2003) 5–12.
[13] D. Deng, H. Guo, X. Chen, H.J. Kong, Characteristics of coherent and incoherent off-axis elegant Hermite–Gaussian beam combinations, J. Opt. A: Pure Appl. Opt. 5 (5) (2003) 489–494.
[14] L. Wang, X. Wang, B. Lü, Propagation properties of partially coherent modified Bessel–Gauss beams, Optik 116 (2005) 65–70.
[15] K. Duan, B. Lü, Propagation of Hermite–Laguerre–Gaussian beams through a paraxial optical *ABCD* system with rectangular hard-edged aperture, Opt. Commun. 250 (1-3) (2005) 1–9.
[16] J. Ji, B. Lü, Matrix formulation of axis-symmetric laser beams through paraxial *ABCD* system containing hard-edged apertures: a comparative study, Optik 116 (2005) 219–225.
[17] B. Lü, S. Luo, Approximate propagation equations of flattened Gaussian beams passing through a paraxial *ABCD* system with hard-edged aperture, J. Mod. Opt. 48 (15) (2001) 2169–2178.
[18] L. Pan, B. Lü, Propagation properties of partially polarized Gaussian Schell-model beams through and axis-unsymmetric paraxial *ABCD* system, Opt. Quantum Electron. 35 (2003) 129–138.
[19] B. Lü, X. Ji, An approximate analytic study of laser beams with amplitude modulations and phase fluctuations through a multi-apertured *ABCD* system, J. Opt. A: Pure Appl. Opt. 6 (2) (2004) 161–166.
[20] S.A. Collins, Lens-system diffraction integral written in terms of matrix optics, J. Opt. Soc. Am. 60 (9) (1970) 1168–1177.
[21] A. Tovar, L.W. Casperson, Generalized beam matrices: Gaussian beam propagation in misaligned complex optical systems, J. Opt. Soc. Am. A. 12 (7) (1995) 1522–1533.
[22] A. Tovar, L.W. Casperson, Generalized beam matrices, III. Application to diffraction analysis, J. Opt. Soc. Am. A. 13 (11) (1996) 2239–2246.
[23] L.C. Andrews, R.L. Phillips, Laser beam propagation through random media, SPIE Press, Washington, 1998, 268pp.
[24] Y. E. Yenice, H. T. Eyyuboğlu, Y. Baykal, Propagation of cross beams through atmospheric turbulence, Presented at XII Joint International Symposium on Atmospheric and Ocean Optics, Russia, 27–30 June 2005.
[25] S. Gradysteyn, I.M. Ryzhik, Tables of Integrals, Series and Products, Academic Press, New York, 2000, 360pp.